Prediction of the chemical trends of oxygen vacancy levels in binary metal oxides

Wan-Jian Yin, Su-Huai Wei, Mowafak M. Al-Jassim, and Yanfa Yan

Citation: Appl. Phys. Lett. **99**, 142109 (2011); doi: 10.1063/1.3647756
View online: http://dx.doi.org/10.1063/1.3647756
View Table of Contents: http://aip.scitation.org/toc/apl/99/14
Published by the American Institute of Physics

RIGHTSLINK

Prediction of the chemical trends of oxygen vacancy levels in binary metal oxides

Wan-Jian Yin, Su-Huai Wei, Mowafak M. Al-Jassim, and Yanfa Yan[a)]
National Renewable Energy Laboratory, Golden, Colorado 80401, USA

(Received 21 May 2011; accepted 9 September 2011; published online 5 October 2011)

We propose simple principles to predict qualitatively the chemical trends of oxygen vacancy levels in binary metal oxides by analyzing the atomic wavefunction characters of the conduction-band minimum (CBM). We show that if the CBM is a metal-oxygen antibonding state due to either *s-s* coupling, *p-p* coupling, or *p-d* coupling, then, in general, the oxygen vacancy level is deep. The stronger coupling leads to deeper levels. If the CBM is a non-bonding *d* state, then the oxygen vacancy level could be shallow. These principles are confirmed by the calculated trends of oxygen vacancy levels in representative binary metal oxides using hybrid density-functional method. © *2011 American Institute of Physics*. [doi:10.1063/1.3647756]

Conventional metal oxides are chemical compounds containing oxygen and metal elements that have d^0 or d^{10} configurations. Many of these metal oxides, e.g., ZnO, SnO_2, In_2O_3, and TiO_2, play an important role in today's optoelectronic devices and solar cells. Most of the oxides are wide-bandgap, *n*-type semiconductors even though they are not intentionally doped. For quite a long time, it was commonly believed that oxygen vacancies (V_O) in metal oxides are the electron donors because the formation energy of V_O in metal oxides is low and the electrical conductivity of the *n*-type oxides is closely linked to the formation of V_O, e.g., the electrical conductivity varies inversely with oxygen partial pressure.[1–3] However, recent theoretical and experimental studies have put this point of view in question. For example, it has been shown that although V_O is the most stable donor-like defect in ZnO, its (0/2+) transition energy level at around 1 eV (Refs. 4–6) below the conduction-band minimum (CBM) is too deep to generate enough charge carriers at room temperature. Similar calculations have also been done for other important metal oxides such as SnO_2, In_2O_3, and TiO_2, suggesting that V_O transition energy levels may also be deep in SnO_2 and In_2O_3, but is shallow in TiO_2. The situation is further complicated by calculations using different exchange-correlation approximations for the density-functional methods, such as local density approximation (LDA), generalized gradient approximation (GGA), GGA+U, and hybrid density functional. For example, the calculated ionization energy for V_O in ZnO ranges from 0.08 to 2.2 eV (Refs. 4, and 6–8). For SnO_2 and In_2O_3, the calculated ionization energies of V_O are reported to range from −0.5 to 1.8 eV (Refs. 7–10). A wide range of ionization energy of V_O in TiO_2 from −0.4 to 1.46 eV is also reported in the literature.[11–14] Because of the lack of accurate experimental data on these transition energy levels, it is crucial to understand the general chemical trend of V_O levels in metal oxides because such a rational understanding can help us understand the calculated results and improve calculation approaches and provide principles for designing V_O levels according to desired applications.

In this letter, we present simple principles to predict qualitatively the trends of oxygen vacancy levels in binary metal oxides by analyzing the character of the CBM states. In general, we find that the character of a V_O level can be either similar or decoupled from that of the CBM state. If the CBM state is derived from the metal-oxygen antibonding state through either *s–s* coupling (e.g., ZnO, SnO_2, and In_2O_3), *p–p* coupling (e.g., Sb_2O_3 and Bi_2O_3), or *p–d* coupling (ZrO_2 and HfO_2), then the characters of V_O levels are derived mostly from the CBM state. In this case, the V_O levels should be deep, in general. The stronger the coupling, the deeper of the level is. However, if the CBM is a non-bonding *d* state (e.g., anatase TiO_2), the characters of V_O levels are usually *not* derived from CBM. *Only* in this case, the V_O levels could be shallow. Our principles are supported by extensive calculation of V_O levels in representative oxides.

The calculations of defect level and formation energies are performed using density-functional theory (DFT) as implemented in the VASP code[15] using the standard frozen-core projector augmented-wave (PAW) method.[16] The cut-off energy for basis functions is 400 eV. The GGA (Ref. 17) is used for initial structural relaxations and the hybrid density functional (HSE06 (Ref. 18)) is used to do the final structural relaxation and determine the (0/2+) transition energy levels of V_O. In the defect calculation, we use supercells of 160, 64, 72, 80, 108, 160, 80, 126, and 96 atoms for ZnO, CdO, SnO_2, In_2O_3, ZrO_2, TiO_2, Bi_2O_3, and Sb_2O_3. Both the Γ-point and Monkhorst-Park $(2 \times 2 \times 2)$ special k-point grids[19] are used in the HSE06 calculation. For HSE06, the portion of exact exchange energy has been chosen separately for each oxide to correct their bandgaps to experimental values. The details on how to calculate the transition levels of V_O are described in Refs. 20 and 21.

We first discuss the formation mechanism of V_O levels in oxides. The formation of a metal oxide has both ionic and covalent contributions. It can be described schematically as in Fig. 1. The valence states of an individual cation and oxygen are shown in Fig. 1(a). Because the electronic potential is higher for the cation than for oxygen, electrons are transferred from the cation to oxygen; so the cation is positively charged and oxygen is negatively charged. Such a transfer lowers the orbital energy of the cation and raises the orbital

[a)]Present address: Department of Physics and Astronomy, The University of Toledo. Electronic mail: yanfa.yan@utoledo.edu.

 © 2011 American Institute of Physics

RIGHTSLINK

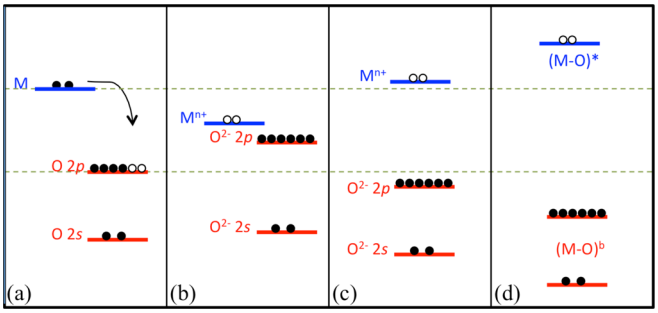

FIG. 1. (Color online) Schematic plot of the metal cation (M^{n+}) and oxygen energy-level evolution in metal oxides. (a) atomic energy level; (b) after the charge transfer between cation and oxygen; (c) after the inter-atomic Coulomb repulsion; and (d) after the covalent energy-level repulsion.

energy of the oxygen due to intra-atomic Coulomb repulsion [Fig. 1(b)]. Next, when the cation and oxygen are pulled together to form a crystal, the inter-atomic Coulomb interaction pushes the cation level higher in energy and lowers the energy levels of oxygen [Fig. 1(c)]. The symmetry-allowed coupling between the cation orbitals and the anion orbitals further shift the antibonding cation orbital upward in energy and lower the oxygen bonding orbital energy [Fig. 1(d)], thus forming a partially covalent bond. In this case, the CBM is usually formed by a cation–oxygen antibonding state and the highest occupied orbital, usually with mainly the oxygen *p* character, forms the VBM. In some cases involving metals with *d* orbitals, due to symmetry constrain, the CBM is derived from *d* nonbonding states. In these cases, the CBM will be close to the cation orbital energy shown in Fig 1(c) and the cation antibonding state has a higher energy. With the above understanding, we can divide metal oxides into two categories depending on how the CBMs are derived: either from cation-oxygen antibonding states or cation *d* nonbonding states. The first category includes *s*-*s* orbital coupling (type-*s* oxides), *p*-*p* orbital coupling (type-*p* oxides), and *p*-*d* orbital (type-d_{ab} oxides). The second category includes cations with *d* orbitals (type-d_{nb}) and usually has high symmetry.

For type-*s* oxides such as ZnO, CdO, In_2O_3, and SnO_2, the cation *s* orbital is nominally unoccupied. The coupling between cation *s* and O 2*s* orbitals pushes the cation *s* orbital to higher energy and forms the CBM state. When a V_O is formed, i.e., an oxygen atom is removed, dangling bonds are form at the surrounding cation sites. Because the inter-atomic Coulomb repulsion and symmetry-allowed energy-level repulsion associated with the removed O atom is also removed, a state associated with the dangling bonds drops from the CBM, forming the V_O state. It has two electrons from the cation atoms surrounding the removed O atom site. Figure 2(a) shows the example schematically in ZnO. How much the state would drop from CBM depends on the cation-oxygen *s*-*s* coupling, which is usually quite strong in type-*s* oxides. Thus, neutral V_O levels are in general deep for type-*s* oxides. Moreover, because the cation-anion coupling [Figs. 1(c) and 1(d)] are usually larger if the cation-anion bond length is smaller, we would expect the V_O level to be deeper, i.e., the ionization energy E_i will be larger, if the cation ionic size is smaller. To test this idea, we have systematically calculated the (0/2+) ionization energies of V_O

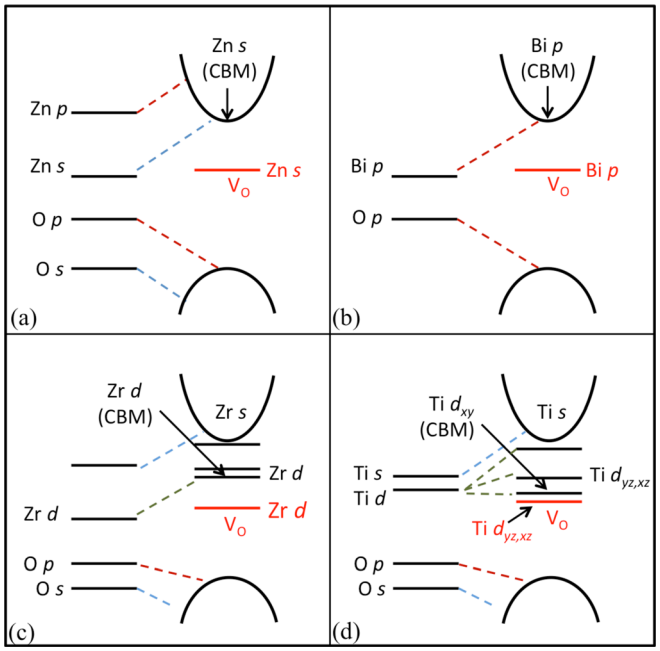

FIG. 2. (Color online) The schematic demonstration of the formation mechanisms of V_O state and the CBM in different types of oxides. (a) ZnO, (b) Bi_2O_3, (c) ZrO_2, and (d) TiO_2 are chosen as representative examples of type-*s*, type-*p*, type-d_{ab}, and type-d_{nb} oxides. The neutral V_O levels in the figures are labeled by V_O. The main chemical characters of V_O states and CBM are also indicated.

in type-*s* oxides, ZnO, SnO_2, In_2O_3, and CdO. The results are shown in Table I. Note that for all the metal oxides studied here, we find that V_O is a negative U defect, i.e., the transition to V_O^{1+} is unstable. We see from Table I that, indeed, the transition energies are generally deep in these oxides, and the V_O (0/2+) ionization energy decreases consistently from ZnO to SnO_2 to In_2O_3 to CdO, following the trend of cation-oxygen bond length from Zn-O to Sn-O to In-O to Cd-O. To test how the coupling strength affects the V_O level, we have calculated the V_O (0/2+) ionization energies in ZnO by changing the lattice constant of ZnO. We find that the V_O (0/2+) level is increased to 1.95 eV when the lattice constant is reduced by 2%, whereas it is decreased to 0.78 eV when the lattice constant is expanded by 2%.

There are only a few type-*p* oxides, such as SnO, PbO, Sb_2O_3, and Bi_2O_3, where cation *s* orbitals are fully occupied inside the valence band and behave more like a semicore

TABLE I. The HSE06 calculated direct bandgap at Γ E_g^{hyb} and (0/2+) electron ionization energy, E_i(0/2+), of V_O in various oxides. The experimental bandgap E_g^{exp} and the cation-oxygen bond length L are also given.

	E_i(0/2+) (eV)	E_g^{hyb} (eV)	E_g^{exp} (eV)	L (Å)
ZnO	1.15	3.45	3.41	1.98
SnO_2	0.73	3.52	3.61	2.07
In_2O_3	0.57	2.76	2.81	2.21
CdO	0.47	2.27	2.28	2.36
Sb_2O_3	1.68	3.49	3.3	2.01
Bi_2O_3	1.03	2.73	2.6–2.8	2.16
TiO_2	−0.38	3.02	3.1	1.94
ZrO_2	1.48	4.60	~5.0	2.14
HfO_2	1.46	5.16	5.68	2.12

RIGHTSLINK

state. For these oxides, the CBM is derived from the antibonding cation *p* orbital. When an oxygen atom is removed from the lattice, the V_O dangling bond state is also derived from the cation *p* orbitals. Figure 2(b) shows the example schematically of V_O in Bi_2O_3. Because the situation is similar between type-*p* metal oxides and type-*s* metal oxides, we also expect that the V_O (0/2+) transition energy level below the CBM will be deeper and the ionization energy E_i will be larger if the cation ionic size is smaller. Table I shows the calculated results for two type-*p* oxides, Sb_2O_3 and Bi_2O_3. Again, we can see that the trend of ionization energies follows the trend of cation size.

For type-d_{ab} oxides, their low symmetries usually allow significant oxygen *p* and cation *d* coupling. Taking monoclinic ZrO_2 as an example, Zr has an $[Kr]4d^25s^2$ configuration with 5*s* orbital higher in energy than 4*d*. Its CBM is derived by the Zr 4*d* and O 2*p* antibonding state. As in type-*s* and type-*p* oxides, when a V_O is formed, the inter-atomic Coulomb repulsion and symmetry-allowed energy-level repulsion associated with this O atom are removed. Therefore, the V_O state, which is derived from the coupled Zr 4*d* state, now dropped much below the CBM, as shown in Fig. 2(c). This picture is confirmed by our calculated transition energy for V_O in monoclinic ZrO_2. The calculated E(0/2+) is 1.48 eV. Our calculation indicates that V_O in monoclinic HfO_2 is also very deep. The trends are consistent with previous calculations.[22,23]

For type-d_{nb} oxides, the CBM is derived mostly from the cation *d* nonbonding states due to symmetry constraint. Taking anatase TiO_2 as an example, Ti has an $[Ar]3d^24s^2$ configuration. The Ti 4*s* orbital is delocalized; thus, it couples strongly with the O 2*s* orbital, which upshifts the Ti 4*s*-derived conduction-band state to a high energy. Because Ti is sitting at a distorted octahedral center with a local D_{2d} symmetry, the low-energy crystal field split t_{2g} *d* states further into d_{xy} states and doubly degenerated d_{yz}/d_{xz} states. At the Brillouin zone center, only the doubly degenerated d_{yz}/d_{xz} states couple significantly with O *s* and *p* orbitals and the $3d_{xy}$ remains as a nonbonding orbital. Therefore, after forming TiO_2, nonbonding Ti $3d_{xy}$ state becomes the CBM of TiO_2. When a V_O is generated, the Ti 4*s* derived dangling-bonds state, which had stronger coupling with the O 2*s* state, drops to a position slightly above CBM. The doubly degenerated d_{yz}/d_{xz}-derived dangling-bond state will drop also. Because the distortion-induced crystal field splitting is not significant in anatase TiO_2, the energy difference between Ti $3d_{xy}$ states and Ti $3d_{yz}/d_{xz}$ states is not significant. Therefore, the doubly degenerated d_{yz}/d_{xz}-derived dangling-bond state drops to a position very close to the Ti $3d_{xy}$-derived CBM state, forming a shallow defect level. The situation is described schematically in Fig. 2(d). Our HSE calculations show that the neutral Vo level is about 0.22 eV below the CBM and the transition level $\epsilon(0/+2)$ of V_O in TiO_2 is above the CBM—in part, because of the large cation displacement around the V_O site.[11] Thus, V_O is indeed a shallow donor in TiO_2. We should point out that the type-d_{nb} oxides may not always lead to shallow V_O levels. It could have deep levels if the antibonding states are close to the nonbonding state and the anion-cation coupling is large.

In conclusion, we have presented general principles to predict qualitatively the chemical trends of V_O levels in binary metal oxides by analyzing the character of the CBM of oxides. We have proposed that in type-*s,* type-*p*, and type-d_{ab} oxides, V_O states and the CBMs are derived from the same antibonding states. Therefore, the V_O levels are generally deep. The V_O levels depend on the coupling strength—the stronger coupling leads to deeper levels. Shallow V_O levels may exist in type-d_{nb} oxides, if the antibonding *s* or/and *p* states are much higher in energy than the nonbonding *d*-derived CBM and the anion-cation coupling is weak. These principles provide a validity check of the numerically calculated results and guidance for searching for oxides that can have shallow V_O levels.

This work was supported by the U.S. Department of Energy under Contract No. DE-AC36-08GO28308.

[1]*Metal Oxides: Chemistry and Applications*, edited by J. L. G. Fierro (CRC, New York, 2006).
[2]C. N. R. Rao and B. Raveau, *Transition Metal Oxides: Structure, Properties, and Synthesis of Ceramic Oxides* (Wiley, New York, 1998).
[3]D. M. Smyth, *The Defect Chemistry of Metal Oxides* (Oxford University Press, London, 2000).
[4]A. Janotti and C. G. Van de Walle, Appl. Phys. Lett. **87**, 122102 (2005).
[5]F. A. Selim, M. H. Weber, D. Solodovnikov, and K. G. Lynn, Phys. Rev. Lett. **99**, 085502 (2007).
[6]F. Oba, A. Togo, I. Tanaka, J. Paier, and G. Kresse, Phys. Rev. B **77**, 245202 (2008).
[7]S. Lany and A. Zunger, Phys. Rev. Lett. **98**, 045501 (2007).
[8]P. Agoston, K. Albe, R. M. Nieminen, and M. J. Puska, Phys. Rev. Lett. **103**, 245501 (2009).
[9]C. Kilic and A. Zunger, Phys. Rev. Lett. **88**, 095501 (2002).
[10]A. K. Singh, A. Janotti, M. Scheffler, and C. G. Van de Walle, Phys. Rev. Lett. **101**, 055502 (2008).
[11]A. Janotti, J. B. Varley, P. Rinke, N. Umezawa, G. Kresse, and C. G. Van de Walle, Phys. Rev. B. **81**, 085212 (2010).
[12]J. Osorio-Guillen, S. Lany, and A. Zunger, Phys. Rev. Lett. **100**, 036601 (2008).
[13]B. J. Morgan and G. W. Watson, Phys. Rev. B. **80**, 233102 (2009).
[14]E. Finazzi, C. Di Valentin, G. Pacchioni, and A. Selloni, J. Chem. Phys. **129**, 154113 (2008).
[15]G. Kresse and J. Furthmuller, Phys. Rev. B **54**, 11169 (1996); Comput. Mater. Sci. **6**, 15 (1996).
[16]P. E. Blochl, Phys. Rev. B **50**, 17953 (1994); G. Kresse and D. Joubert, *ibid.* **59**, 1758 (1999).
[17]J. P. Perdew and Y. Wang, Phys. Rev. B **45**, 13244 (1992).
[18]J. Heyd, G. E. Scuseria, and M. Ernzerhof, J. Chem. Phys. **118**, 8207 (2003); J. Paier, M. Marsman, K. Hummer, G. Kresse, I. C. Gerber, and J. G. Ángyán, J. Chem. Phys. **124**, 154709 (2006).
[19]H. J. Monkhorst and J. D. Pack, Phys. Rev. B **13**, 5188 (1976).
[20]S.-H. Wei, Comput. Mater. Sci. **30**, 337 (2004); Y. Yan and S.-H. Wei, Phys. Status Solidi B **245**, 641 (2008).
[21]C. G. van de Walle and J. Neugebauer, J. Appl. Phys. **95**, 3851 (2004).
[22]A. S. Foster, V. B. Sulimov, F. L. Gejo, A. L. Shluger, and R. M. Nieminen, Phys. Rev. B **64**, 224108 (2001).
[23]E.-A. Choi and K. J. Chang, Appl. Phys. Lett. **94**, 122901 (2009).

RIGHTSLINK